

Coherent imaging without phases

Miguel Moscoso *

* Joint work with Alexei Novikov Chrysoula Tsogka and George Papanicolaou

Waves and Imaging in Random Media, September 2017

Outline

- 1 The phase retrieval problem
- 2 A convex approach
- 3 Illumination strategies
- 4 Conclusions

Motivation

In many situations it is difficult, or impossible, to measure the phases.

Only the intensities are available for imaging!

- X-ray cristalography
- THz radar & imaging systems
- Diffraction imaging
- Astronomical imaging
- ...

Motivation

In many situations it is difficult, or impossible, to measure the phases.

Only the intensities are available for imaging!

- X-ray cristalography
- THz radar & imaging systems
- Diffraction imaging
- Astronomical imaging
- ...

COHERENT WAVE PROPAGATION

The significance of phase



Figure: Atletico de Madrid soccer shield (top) and Real Madrid soccer shield (bottom).

Motivation

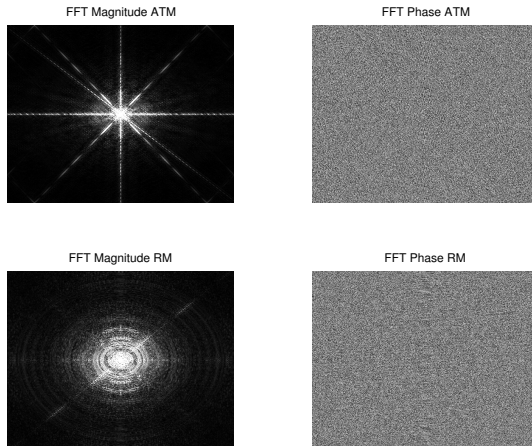


Figure: Magnitudes and phases of Atletico (top row) and Real Madrid (bottom row) soccer shields.

Motivation

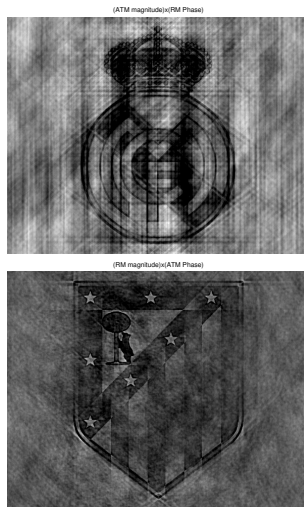


Figure: It's not about the intensity. What matters is the phase!!

The phase retrieval problem

Mathematically ...

... the phase retrieval problem consists of recovering an unknown signal $x[n]$ from the amplitude $|\hat{x}[k]|$ of its Fourier transform

$$\hat{x}[k] = \sum_{n=1}^N x[n] e^{-i2\pi kn/N}, \quad k = 1, \dots, N.$$

The phase retrieval problem

Mathematically ...

... **the phase retrieval problem** consists of finding the phases that satisfy a set of linear constraints for the measured amplitudes

$$| \langle x, a_k \rangle |^2 = |b_k|^2.$$

The phase retrieval problem: algorithms



R.W. Gerchberg and W.O. Saxton, *A practical algorithm for the determination of phase from image and diffraction plane pictures*, Optik 35, 237-246 (1972).



J.R. Fienup, *Reconstruction of an object from the modulus of its Fourier transform*, Optics Letters 3, 27-29 (1978).

*Project a guess image to the spatial domain and frequency domain **alternatively**, and **use the known information** of the original image to modify the projection in each step.*

The phase retrieval problem: algorithms



R.W. Gerchberg and W.O. Saxton, *A practical algorithm for the determination of phase from image and diffraction plane pictures*, Optik 35, 237-246 (1972).



J.R. Fienup, *Reconstruction of an object from the modulus of its Fourier transform*, Optics Letters 3, 27-29 (1978).

Project a guess image to the spatial domain and frequency domain **alternatively**, and **use the known information** of the original image to modify the projection in each step.

These algorithms require image prior and convergence is not guarantee!!!

The phase retrieval problem

Goal: To devise other approaches that guarantee convergence to the exact solution without prior information.

The phase retrieval problem

Assume that imaging can be formulated as a linear inverse problem

$$\mathcal{A}_{\hat{f}} \rho = b_{\hat{f}}.$$

The phase retrieval problem

Assume that imaging can be formulated as a linear inverse problem

$$\mathcal{A}_{\hat{f}} \boldsymbol{\rho} = \mathbf{b}_{\hat{f}}.$$

Here, $\mathcal{A}_{\hat{f}} \in \mathbb{C}^{N \times K}$ is the model matrix that relates the unknown vector $\boldsymbol{\rho} \in \mathbb{C}^K$ to the data vector $\mathbf{b}_{\hat{f}} \in \mathbb{C}^N$. Usually $N \ll K$!

The phase retrieval problem

Imaging WITH phases

Find $\rho \in \mathbb{C}^K$ from

$$\mathcal{A}_{\hat{f}} \rho = b_{\hat{f}},$$

given the data vector $b_{\hat{f}} \in \mathbb{C}^N$ with both amplitudes and phases.

The phase retrieval problem

When **only the intensities can be recorded**, the data are given by the vector

$$\beta_{\hat{f}} = \text{diag}(\mathbf{b}_{\hat{f}} \mathbf{b}_{\hat{f}}^*) \in \mathbb{R}^N.$$

The phase retrieval problem

When **only the intensities can be recorded**, the data are given by the vector

$$\beta_{\hat{f}} = \text{diag}(\mathbf{b}_{\hat{f}} \mathbf{b}_{\hat{f}}^*) \in \mathbb{R}^N.$$

Imaging WITHOUT phases

The basic equation in intensity-based imaging is

$$\text{diag}(\mathcal{A}_{\hat{f}} \boldsymbol{\rho} \boldsymbol{\rho}^* \mathcal{A}_{\hat{f}}^*) = \beta_{\hat{f}}.$$

This problem is nonlinear, nonconvex in the **vector** $\boldsymbol{\rho} \in \mathbb{C}^K$. ☹

A convex approach

KEY: Replaced the **nonlinear vector** problem by a **linear matrix** one. Introduce

- The decision variable $\mathcal{X} := \rho\rho^* \in \mathbb{C}^{K \times K}$, and the
- operator $L_{\hat{f}} : \mathbb{C}^{K \times K} \rightarrow \mathbb{R}^N$, such that $\mathcal{L}_{\hat{f}}(\mathcal{X}) := \text{diag}(\mathcal{A}_{\hat{f}}\mathcal{X}\mathcal{A}_{\hat{f}}^*)$.

Imaging WITHOUT phases

Then, **at the matrix level**, the equation in intensity-based imaging is

$$\mathcal{L}_{\hat{f}}(\mathcal{X}) = \beta_{\hat{f}}.$$

The quadratic measurements on ρ become linear on $\mathcal{X} := \rho\rho^*$!

A convex approach

Rank minimization

Solve the following **rank minimization** problem

$$\min \text{rank}(\mathcal{X}) \quad \text{subject to} \quad \mathcal{L}_{\hat{f}}(\mathcal{X}) = \beta_{\hat{f}}, \quad \mathcal{X} \geq 0.$$

This problem is still nonconvex!!! ☹

A convex approach

Rank minimization

Solve the following **rank minimization** problem

$$\min \text{rank}(\mathcal{X}) \quad \text{subject to} \quad \mathcal{L}_{\hat{f}}(\mathcal{X}) = \beta_{\hat{f}}, \quad \mathcal{X} \geq 0.$$

This problem is still nonconvex!!! ☹

Relax!

Solve the following **trace minimization** problem

$$\min \text{trace}(\mathcal{X}) \quad \text{subject to} \quad \mathcal{L}_{\hat{f}}(\mathcal{X}) = b_I, \quad \mathcal{X} \geq 0.$$

This makes the problem convex and solvable in polynomial time. ☺

A convex approach



A. Chai, M. Moscoso, G. Papanicolaou, *Array imaging using intensity-only measurements*, Inverse Problems 27 (2011).



E. J. Candes, Y. C. Eldar, T. Strohmer, V. Voroninski, *Phase Retrieval via Matrix Completion*, SIAM Journal on Imaging Sciences 6 (2013).

A convex approach: algorithm

Iterative algorithm for $\min \text{trace}(\mathcal{X})$ s. t. $\mathcal{L}_{\hat{f}}(\mathcal{X}) = \mathbf{b}_I$.

Require: Set $Y_{-1} = Y_0 = 0$ and $t_{-1} = t_0 = 1$, and pick the initial value for step size β .

repeat

 Compute weight $w = \frac{t_{k-1}-1}{t_k}$.

 Compute $W_k = (1 + w)Y_k - wY_{k-1}$.

 Compute the matrix $G = W - \beta \mathcal{L}_{\hat{f}(\omega)}^* (\mathcal{L}_{\hat{f}(\omega)}(W) - \mathbf{b}_I(\omega))$.

 Set $Y_{k+1} = S_\tau(G)$.

 Compute $t_{k+1} = \frac{1 + \sqrt{1 + 4t_k^2}}{2}$.

until Convergence

Gradient descent method with singular value thresholding

$$S_\tau(G) = \hat{U} \text{diag}(\boldsymbol{\sigma} - \tau)^+ \hat{V}^*.$$

A convex approach: algorithm



J.F. Cai, E.J. Candès, and Z. Shen, *A Singular Value Thresholding Algorithm for Matrix Completion*, SIAM J. Optim. 20 (2008).



K.C. Toh and S. Yun, *An accelerated proximal gradient algorithm for nuclear norm regularized least squares problems*, Pacific J. Optimization 6 (2010).

Numerical simulations: active array imaging

Let us consider the problem of active array imaging ...

Schematic for **active** array imaging

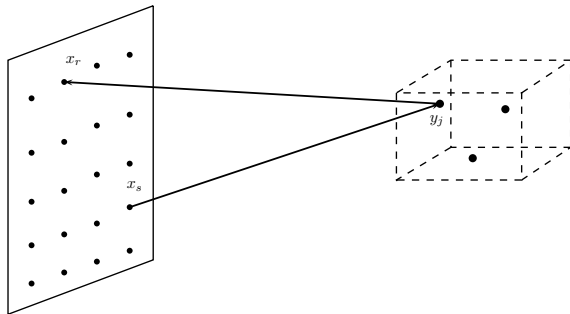
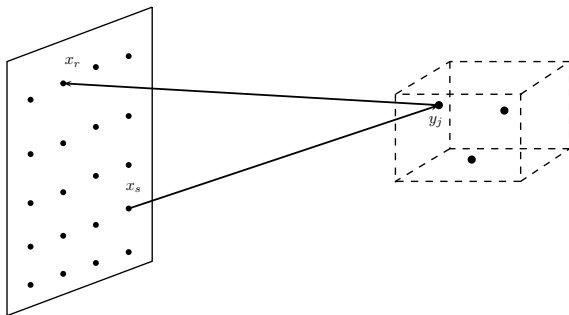


Figure: We want to determine the location and reflectivities of (small or extended) reflectors by sending probing signals from the array and recording the backscattered signals. **Only the intensities are recorded, in our case!**

Data model

We consider a region of interest: the Image Window IW.



We define a grid \mathbf{y}_j , $j = 1, \dots, K$, a discretization of the IW and seek to determine the reflectivities on this grid $\rho_j = \rho(\mathbf{y}_j)$, $j = 1, \dots, K$.

Our unknown is the vector $\boldsymbol{\rho} \in \mathbb{C}^K$,

$$\boldsymbol{\rho} = [\rho_1, \dots, \rho_K]^t \in \mathbb{C}^K, \quad \rho_j = \rho(\mathbf{y}_j), \quad j = 1, \dots, K.$$

The data model

In the **Born approximation**, the response at \mathbf{x}_r due to the signal sent from \mathbf{x}_s is given by

$$\hat{P}_{rs}(\omega) = \sum_{j=1}^K \rho_j \hat{G}_0(\mathbf{x}_r, \mathbf{y}_j, \omega) \hat{G}_0(\mathbf{y}_j, \mathbf{x}_s, \omega),$$

where $\hat{G}_0(\mathbf{x}, \mathbf{y}, \omega) = e^{i\kappa|\mathbf{x}-\mathbf{y}|} / (4\pi|\mathbf{x}-\mathbf{y}|)$.

The data model

In the **Born approximation**, the response at \mathbf{x}_r due to the signal sent from \mathbf{x}_s is given by

$$\hat{P}_{rs}(\omega) = \sum_{j=1}^K \rho_j \hat{G}_0(\mathbf{x}_r, \mathbf{y}_j, \omega) \hat{G}_0(\mathbf{y}_j, \mathbf{x}_s, \omega),$$

where $\hat{G}_0(\mathbf{x}, \mathbf{y}, \omega) = e^{i\kappa|\mathbf{x}-\mathbf{y}|} / (4\pi|\mathbf{x}-\mathbf{y}|)$.

We collect all the data in the **response matrix**

$$\hat{P}(\omega) = [\hat{P}_{rs}(\omega)]_{r,s=1}^N.$$

The data model

If $\hat{\mathbf{f}} = [\hat{f}_1, \dots, \hat{f}_N]^T$ is the **illumination vector**, then the data $\mathbf{b}_{\hat{\mathbf{f}}}$ (including phases!!!) at the array is given by

$$\mathbf{b}_{\hat{\mathbf{f}}} = \hat{P} \hat{\mathbf{f}}.$$

Through $\hat{P} \hat{\mathbf{f}}$, we define the model matrix

$$\mathcal{A}_{\hat{\mathbf{f}}} \boldsymbol{\rho} = \hat{P} \hat{\mathbf{f}},$$

with

$$\left[\mathcal{A}_{\hat{\mathbf{f}}} \right]_{rk} = G(\mathbf{x}_r, \mathbf{y}_k, \omega) \sum_{s=1}^N \hat{f}_s G(\mathbf{y}_k, \mathbf{x}_s, \omega).$$

for $r = 1, \dots, N$, $k = 1, \dots, K$.

Numerical simulations: examples I

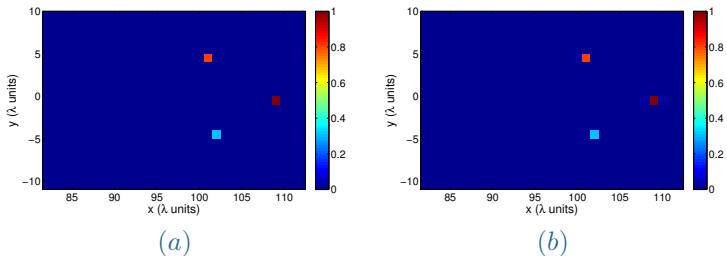
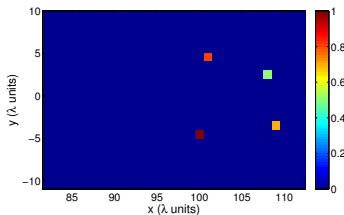


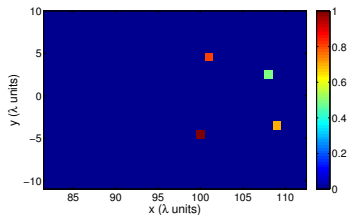
Figure: (a) Original configuration. 21 transducers. 10×10 pixels in IW. Grid points separated by 1. $a/L = 1$. Single illumination. (b) Numerical result by solving trace minimization with **no noise**.

In all the images we normalize the spatial units by λ .

Numerical simulations: examples II



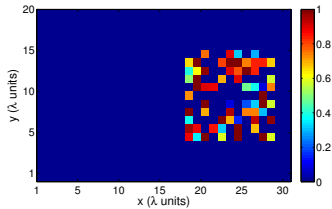
(a)



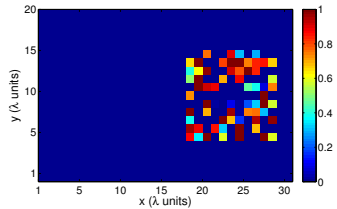
(b)

Figure: Same as before with 4 scatterers. **No noise.**

Numerical simulations: examples III



(a)



(b)

Figure: Same as before with 65 scatterers. **No noise.**

Sparsity is not required!

Numerical simulations: examples IV

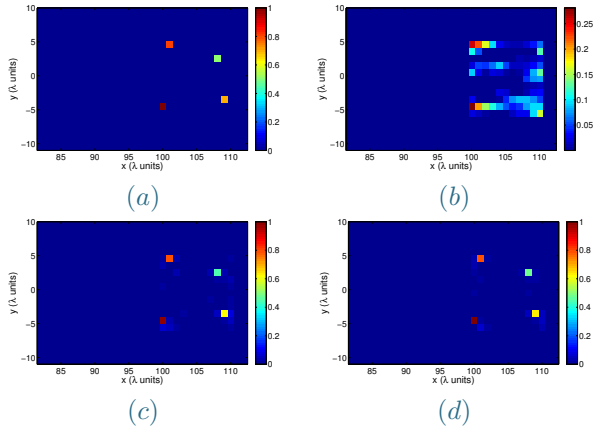


Figure: 0.5% noise. (a) Original configuration. (b) 1 illumination. (c) 5 illuminations. (d) 10 illuminations.

The number of illuminations is increased to make the method robust.

A convex approach

Goal accomplished: The method guarantees **exact reconstructions** without image prior.

A convex approach

Goal accomplished: The method guarantees **exact reconstructions** without image prior.

Drawback: It is VERY computationally expensive for large scale problems. Images with K of pixels require the solution of a $K \times K$ optimization problem.

A convex approach

Goal accomplished: The method guarantees **exact reconstructions** without image prior.

Drawback: It is VERY computationally expensive for large scale problems. Images with K of pixels require the solution of a $K \times K$ optimization problem.

Next goal: To devise another approach that guarantees convergence to the exact solution and, at the same time, keep the size of the problem small so the solution can be found more efficiently.

The time reversal operator

Main idea

Imaging with intensity-only can be carried out using the time reversal operator

$$\widehat{M} = \widehat{P}^* \widehat{P},$$

which can be obtained from intensity measurements using an appropriate illumination strategy and the **polarization identity**.

The images can be formed using its SVD.

The time-reversal operator with the polarization identity

Note that for a given illumination vector

$$\begin{aligned}\langle \hat{\mathbf{f}}(\omega), \hat{\mathbf{M}}(\omega) \hat{\mathbf{f}}(\omega) \rangle &= \langle \hat{\mathbf{f}}(\omega), \hat{\mathbf{P}}^*(\omega) \hat{\mathbf{P}}(\omega) \hat{\mathbf{f}}(\omega) \rangle \\ &= \langle \hat{\mathbf{P}}(\omega) \hat{\mathbf{f}}(\omega), \hat{\mathbf{P}}(\omega) \hat{\mathbf{f}}(\omega) \rangle = \|\hat{\mathbf{P}}(\omega) \hat{\mathbf{f}}(\omega)\|^2,\end{aligned}$$

so the quadratic form $\hat{\mathbf{M}}(\omega)$ is determined by intensity only measurements.

The time-reversal operator with the polarization identity

Note that for a given illumination vector

$$\begin{aligned}\langle \widehat{\mathbf{f}}(\omega), \widehat{\mathbf{M}}(\omega) \widehat{\mathbf{f}}(\omega) \rangle &= \langle \widehat{\mathbf{f}}(\omega), \widehat{\mathbf{P}}^*(\omega) \widehat{\mathbf{P}}(\omega) \widehat{\mathbf{f}}(\omega) \rangle \\ &= \langle \widehat{\mathbf{P}}(\omega) \widehat{\mathbf{f}}(\omega), \widehat{\mathbf{P}}(\omega) \widehat{\mathbf{f}}(\omega) \rangle = \|\widehat{\mathbf{P}}(\omega) \widehat{\mathbf{f}}(\omega)\|^2,\end{aligned}$$

so the quadratic form $\widehat{\mathbf{M}}(\omega)$ is determined by intensity only measurements. Use the polarization identity

$$2\langle \mathbf{x}, \mathbf{y} \rangle = \|\mathbf{x} + \mathbf{y}\|^2 - \|\mathbf{x}\|^2 - \|\mathbf{y}\|^2 + \mathbf{i} (\|\mathbf{x} - i\mathbf{y}\|^2 - \|\mathbf{x}\|^2 - \|\mathbf{y}\|^2).$$

The time-reversal operator with the polarization identity

The i -th entry in the diagonal M_{ii} is just the total power received at the array when only the i -th transducer fires a signal.

The off-diagonal terms M_{ij} , $i \neq j$ can be found as follows:

$$\operatorname{Re}(M_{ij}(\omega)) = \operatorname{Re}(M_{ji}(\omega)) = \frac{1}{2} \left(\|\hat{\mathbf{P}}(\omega)\hat{\mathbf{e}}_{i+j}\|^2 - \|\hat{\mathbf{P}}(\omega)\hat{\mathbf{e}}_i\|^2 - \|\hat{\mathbf{P}}(\omega)\hat{\mathbf{e}}_j\|^2 \right)$$

$$\operatorname{Im}(M_{ij}(\omega)) = -\operatorname{Im}(M_{ji}(\omega)) = \frac{1}{2} \left(\|\hat{\mathbf{P}}(\omega)\hat{\mathbf{e}}_{i-j}\|^2 - \|\hat{\mathbf{P}}(\omega)\hat{\mathbf{e}}_i\|^2 - \|\hat{\mathbf{P}}(\omega)\hat{\mathbf{e}}_j\|^2 \right)$$

using the illumination vectors $\hat{\mathbf{e}}_{i+j} = \hat{\mathbf{e}}_i + \hat{\mathbf{e}}_j$ and $\hat{\mathbf{e}}_{i-j} = \hat{\mathbf{e}}_i - \hat{\mathbf{e}}_j$.

Conclusion: With enough illuminations (N^2 of them) we can obtain $\widehat{\mathbf{M}}(\omega)$. Since only the total power received at the array is involved, the method very robust.

Imaging without phases

Key ideas:

(i) The time reversal matrix $\widehat{M} = \widehat{P}^* \widehat{P}$ and \widehat{P} , share the same right singular vectors.

$$\widehat{P}(\omega) = \widehat{U}(\omega) \Sigma(\omega) \widehat{V}^*(\omega) = \sum_{j=1}^{\tilde{M}} \sigma_j(\omega) \widehat{U}_j(\omega) \widehat{V}_j^*(\omega),$$

$$\widehat{M}(\omega) = \widehat{V}(\omega) \Sigma^2(\omega) \widehat{V}^*(\omega) = \sum_{j=1}^{\tilde{M}} \sigma_j^2(\omega) \widehat{V}_j(\omega) \widehat{V}_j^*(\omega).$$

Imaging without phases

Key ideas:

- (i) The time reversal matrix $\widehat{M} = \widehat{P}^* \widehat{P}$ and \widehat{P} , share the same right singular vectors. Hence,
- MUSIC can be applied, without any modification, once \widehat{M} has been obtained.

MUSIC algorithm

A scatterer location corresponds to a peak of the functional

$$\mathcal{I}(\mathbf{y}_s) = \frac{1}{\sum_{j=M+1}^N |\widehat{\mathbf{g}}_0^T(\mathbf{y}_s) \widehat{V}_j|^2}, \quad s = 1, \dots, K.$$

Imaging without phases

Key ideas:

(i) The time reversal matrix $\widehat{\mathbf{M}} = \widehat{\mathbf{P}}^* \widehat{\mathbf{P}}$ and $\widehat{\mathbf{P}}$, share the same right singular vectors. Hence,

- MUSIC can be applied, without any modification, once $\widehat{\mathbf{M}}$ has been obtained.
- Use the right singular vectors of $\widehat{\mathbf{M}}$ as illumination vectors, then the data on the array is known up to a global phase.

$$\widehat{\mathbf{P}}^*(\omega) \widehat{\mathbf{U}}_j(\omega) = \sigma_j(\omega) \widehat{\mathbf{V}}_j(\omega), \quad \widehat{\mathbf{P}}(\omega) \widehat{\mathbf{V}}_j(\omega) = \sigma_j(\omega) \widehat{\mathbf{U}}_j(\omega), \quad j = 1, \dots, N.$$

Since $\widehat{\mathbf{P}}(\omega)$ is complex-valued but symmetric, then $\widehat{\mathbf{U}}_j(\omega) = e^{i\theta_j} \widehat{\mathbf{V}}_j(\omega)$. Hence,

$$\widehat{\mathbf{P}}(\omega) \widehat{\mathbf{V}}_j(\omega) = \sigma_j(\omega) e^{i\theta_j} \overline{\widehat{\mathbf{V}}_j(\omega)}, \quad j = 1, \dots, N,$$

for an unknown global phase $e^{i\theta_j}$ which is different for each $\widehat{\mathbf{V}}_j(\omega)$.

Then, use optimization-based imaging methods to exploit the sparsity of the scatterers in the IW.

Imaging without phases

Advantages:

- Simple and efficient
- Does not need prior information
- Guarantees exact recovery in the noise-free case
- It is robust with respect to additive noise.

Imaging without phases

Advantages:

- Simple and efficient
- Does not need prior information
- Guarantees exact recovery in the noise-free case
- It is robust with respect to additive noise.

Drawback: The data acquisition process is expensive (N^2)... but can be minimized

- using matrix completion, or
- edge illuminations, or

Imaging without phases

Advantages:

- Simple and efficient
- Does not need prior information
- Guarantees exact recovery in the noise-free case
- It is robust with respect to additive noise.

Drawback: The data acquisition process is expensive (N^2)... but can be minimized

- using matrix completion, or
- edge illuminations, or
- instead use the intensities at each receiver ($3N - 2$), or
- Fresnel and Fraunhofer regimes (exactly 6).

Imaging without phases

Advantages:

- Simple and efficient
- Does not need prior information
- Guarantees exact recovery in the noise-free case
- It is robust with respect to additive noise.

Drawback: The data acquisition process is expensive (N^2)... but can be minimized

- using matrix completion, or
- edge illuminations, or
- instead use the intensities at each receiver ($3N - 2$), or
- Fresnel and Fraunhofer regimes (exactly 6).

Corollary (Fraunhofer): A "vector" can be determined from the absolute value of its Fourier coefficients (its DFT) if six versions of it are known, regardless of its size.

Imaging without phases



A. Novikov, M. Moscoso, and G. Papanicolaou, *Illumination Strategies for Intensity-Only Imaging*, SIAM Journal on Imaging Sciences 8 (2015).



M. Moscoso, A. Novikov, and G. Papanicolaou, *Coherent Imaging without Phases*, SIAM Journal on Imaging Sciences 9 (2016).

Numerical experiments

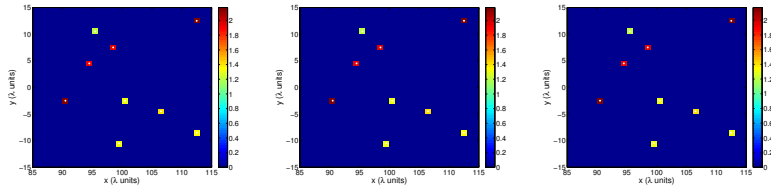


Figure: Noiseless data. Reference image (left), MUSIC (middle), MMV formulation (right). IW of size $30\lambda \times 30\lambda$ which is at a distance $L = 100\lambda$ from the linear array. 100 transducers one wavelength λ apart.

Numerical experiments

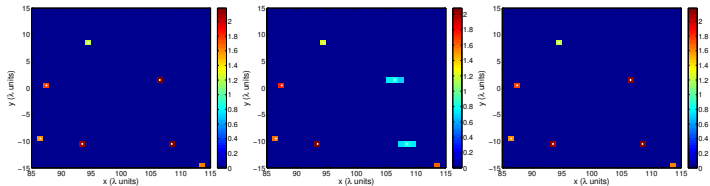


Figure: Same as previous figure but with 10% noise.

Numerical experiments

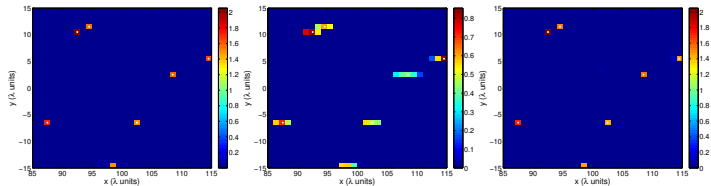


Figure: Same as previous figure but with 20% noise.

Multiple frequency imaging

Imaging with \widehat{M} at a single frequency is not robust relative to small perturbations in the unknown phases.

Multiple frequency imaging

Imaging with \widehat{M} at a single frequency is not robust relative to small perturbations in the unknown phases. We can image robustly if we have interferometric data (Borcea-Papanicolaou-Tsogka 05',06')

$$d((\vec{x}_r, \vec{x}_{r'}), (\vec{x}_s, \vec{x}_{s'}), (\omega, \omega')) = \overline{P(\vec{x}_r, \vec{x}_s; \omega)} P(\vec{x}_{r'}, \vec{x}_{s'}; \omega'),$$

and image interferometrically using

$$\begin{aligned} \mathcal{I}^{CINT}(\vec{y}^s) &= \sum_{\substack{\vec{x}_s, \vec{x}_{s'} \\ |\vec{x}_s - \vec{x}_{s'}| \leq X_d}} \sum_{\substack{\vec{x}_r, \vec{x}_{r'} \\ |\vec{x}_r - \vec{x}_{r'}| \leq X_d}} \sum_{\substack{\omega_l, \omega_{l'} \\ |\omega_l - \omega_{l'}| \leq \Omega_d}} d((\vec{x}_r, \vec{x}_{r'}), (\vec{x}_s, \vec{x}_{s'}), (\omega_l, \omega_{l'})) \\ &\quad \times G_0(\vec{x}_r, \vec{y}^s; \omega_l) G_0(\vec{x}_s, \vec{y}^s; \omega_l) \overline{G_0(\vec{x}_{r'}, \vec{y}^s; \omega_{l'})} G_0(\vec{x}_{s'}, \vec{y}^s; \omega_{l'}). \end{aligned}$$

Remark: Robustness comes at the cost of loss in resolution: $\lambda_0 L/a \rightarrow \lambda_0 L/X_d$ in cross-range, and $c_0/B \rightarrow c_0/\Omega_d$ in range.

Multiple frequency imaging

Imaging with $\widehat{\mathbf{M}}$ at a single frequency is not robust relative to small perturbations in the unknown phases. We can image robustly if we have interferometric data (Borcea-Papanicolaou-Tsogka 05',06')

$$d((\vec{x}_r, \vec{x}_{r'}), (\vec{x}_s, \vec{x}_{s'}), (\omega, \omega')) = \overline{P(\vec{x}_r, \vec{x}_s; \omega)} P(\vec{x}_{r'}, \vec{x}_{s'}; \omega'),$$

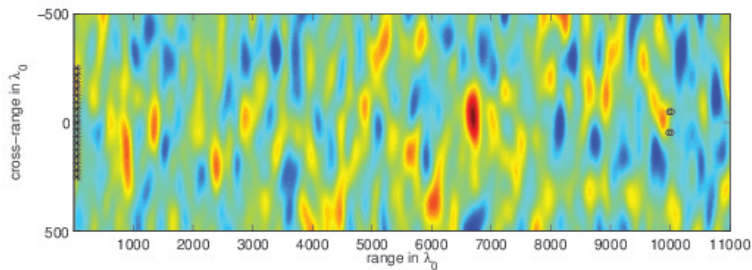
and image interferometrically using

$$\begin{aligned} \mathcal{I}^{CINT}(\vec{y}^s) &= \sum_{\substack{\vec{x}_s, \vec{x}_{s'} \\ |\vec{x}_s - \vec{x}_{s'}| \leq X_d}} \sum_{\substack{\vec{x}_r, \vec{x}_{r'} \\ |\vec{x}_r - \vec{x}_{r'}| \leq X_d}} \sum_{\substack{\omega_l, \omega_{l'} \\ |\omega_l - \omega_{l'}| \leq \Omega_d}} d((\vec{x}_r, \vec{x}_{r'}), (\vec{x}_s, \vec{x}_{s'}), (\omega_l, \omega_{l'})) \\ &\quad \times G_0(\vec{x}_r, \vec{y}^s; \omega_l) G_0(\vec{x}_s, \vec{y}^s; \omega_l) \overline{G_0(\vec{x}_{r'}, \vec{y}^s; \omega_{l'})} G_0(\vec{x}_{s'}, \vec{y}^s; \omega_{l'}). \end{aligned}$$

Or, restricting the data to a single receiver, using

$$\begin{aligned} \mathcal{I}^{SRINT}(\vec{y}^s) &= \sum_{\substack{\vec{x}_s, \vec{x}_{s'} \\ |\vec{x}_s - \vec{x}_{s'}| \leq X_d}} \sum_{\substack{\omega_l, \omega_{l'} \\ |\omega_l - \omega_{l'}| \leq \Omega_d}} d((\vec{x}_r, \vec{x}_r), (\vec{x}_s, \vec{x}_{s'}), (\omega_l, \omega_{l'})) \\ &\quad \times G_0(\vec{x}_r, \vec{y}^s; \omega_l) G_0(\vec{x}_s, \vec{y}^s; \omega_l) \overline{G_0(\vec{x}_r, \vec{y}^s; \omega_{l'})} G_0(\vec{x}_{s'}, \vec{y}^s; \omega_{l'}). \end{aligned}$$

Numerical experiments: random medium



- One realization of the random medium (correlation length $l = 100\lambda_0$, strength of the fluctuations $\sigma = 4 \cdot 10^{-4}$).
- Measurements are for multiple frequencies covering a total bandwidth of 120THz centered at $f_0 = 600$ THz.
- Array size $a = 500\lambda_0$ (0.25 mm) with $N = 81$ array elements, and distance to the IW $L = 10000\lambda_0$ (5mm depth).

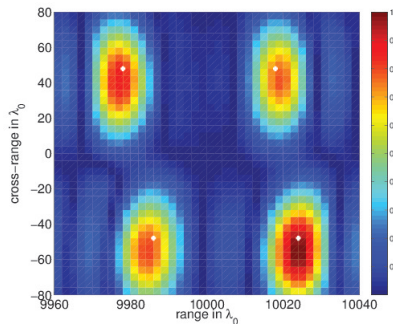
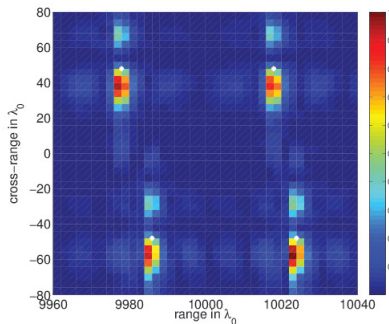
Weak random medium

- The random fluctuations of the wave speed are modeled as

$$\frac{1}{c^2(\mathbf{x})} = \frac{1}{c_0^2} \left(1 + \sigma \mu\left(\frac{\mathbf{x}}{l}\right) \right).$$

- c_0 denotes the average speed
- σ denotes the strength of the fluctuations with correlation length l
- $\mu(\cdot)$ is a stationary random process with zero mean and normalized autocorrelation function $R(|\mathbf{x} - \mathbf{x}'|) = \mathbb{E}(\mu(\mathbf{x})\mu(\mathbf{x}'))$, so that $R(0) = 1$, and $\int_0^\infty R(r)r^2 dr < \infty$.
- We use the random phase model which characterizes wave propagation in the high-frequency regime in random media with weak fluctuations $\sigma \ll 1$ and large correlation lengths l compared to the wavelength λ .

Imaging results random medium

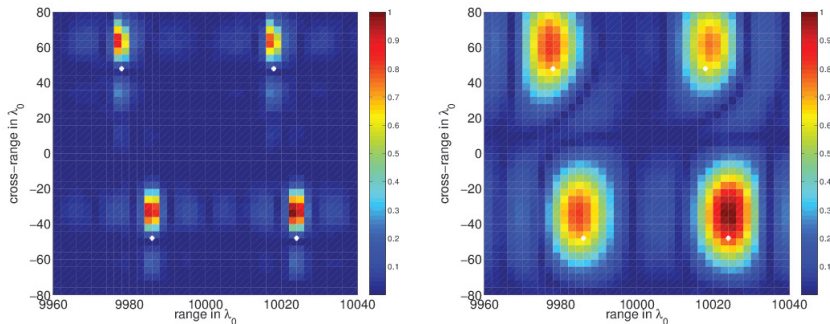


46 equally spaced frequencies in $B = [540, 660]$ THz.

Left: $\Omega_d = B$, $X_d = a$. **Right:** $\Omega_d = 0.12B$, $X_d = 0.25a$.

Robust, statistically stable images are obtained with, however, reduced resolution.

Imaging results random medium



46 equally spaced frequencies in $B = [540, 660]$ THz.

Left: $\Omega_d = B$, $X_d = a$. **Right:** $\Omega_d = 0.12B$, $X_d = 0.25a$.

Robust, statistically stable images are obtained with, however, reduced resolution.

Multiple frequency imaging



M. Moscoso, A. Novikov, G. Papanicolaou, and C. Tsogka, *Multifrequency Interferometric Imaging with Intensity-Only Measurements*, SIAM Journal on Imaging Sciences 10 (2017).

Statistical Stability

Reducing the data to nearby sources and nearby frequencies gives statistically stability with respect to perturbations in the phases.

SRINT is equivalent to CINT for one receiver (which assumes phases are recorded).



L. Borcea, G. Papanicolaou and C. Tsogka, *Interferometric array imaging in clutter*, Inverse Problems 21 (2005).



L. Borcea, G. Papanicolaou and C. Tsogka, *Adaptive interferometric imaging in clutter and optimal illumination*, Inverse Problems 22 (2006).



L. Borcea, G. Papanicolaou and C. Tsogka., *Coherent interferometric imaging in clutter*, Geophysics 71 (2006).



L. Borcea, J. Garnier, G. Papanicolaou and C. Tsogka, *Enhanced statistical stability in coherent interferometric imaging*, Inverse Problems 27 (2011).

Concluding remarks

- The convex approach guarantees exact recovery but it is not feasible for large scale problems.
- Array imaging with intensities only in homogeneous media can be as good as imaging with full information if we control the illuminations. Illumination diversity is the key.
- In weak random media, imaging with intensities-only using single receiver is stable. We use interferometric data so medium-induced phase perturbations cancel for nearby frequencies and illuminations.
- As a special case, we know how to recover exactly a vector from the absolute values of six versions of its DFT, in the imaging context, regardless of its size.

Concluding remarks

Thanks!